NSF-University Wyoming Supercomputer Center
DOE BER SCIDAC

NASA Physical Oceanography:
NNX16AH60G

What drives ocean heat content variability in CESM in the extra-tropics, and at what scales?

Justin Small
Stu Bishop (NCSU), Frank Bryan
Bob Tomas

Acknowledging: Sarah Larson (UWis)
J. Brent Roberts (NASA Goddard/ SEAFLUX)
Lisan Yu (WHOI/OAFLUX)
Kubota-san, Tomita-san (Tokai Uni., Nagoya Uni., J-OFURO)
CESM developers & ASD team

Recap: Relationship between SST and surface turbulent heat flux

correlation of SST and surface latent heat flux.

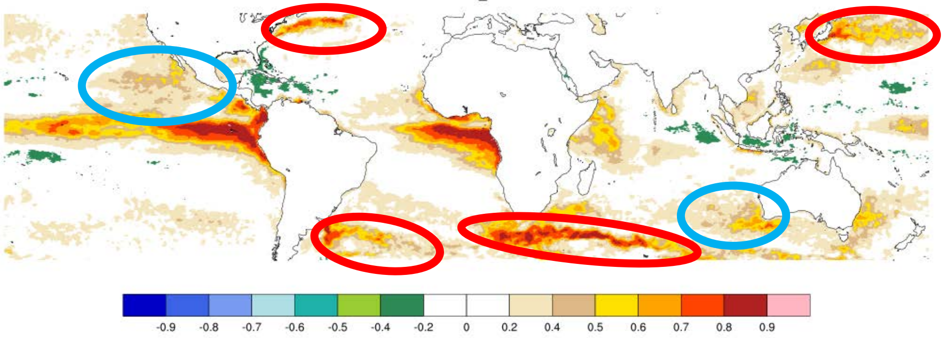

Positive values: ocean drives surface heat flux

correlation of SST *tendency* and surface latent heat flux.

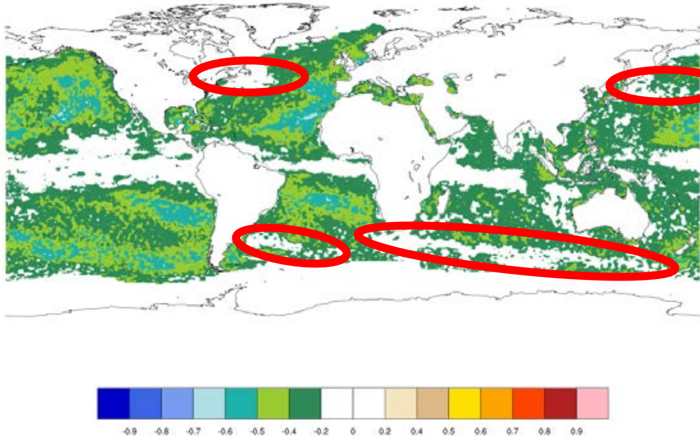

Negative values: atmosphere forces ocean SST

Data from observational product:
J-OFURO-v3 years 2002-2012

Strong positive correlations in ocean frontal/eddy regions (red circled) and also weaker ocean forcing in open ocean (e.g. blue circles) and Tropics

From Bishop et al 2017

Stochastic model of air-sea interaction

- Frankignoul, Hasselmann 1977
- Barsugli and Battisti 1998
- Wu et al. 2006
- Zhang et al 2017

$$\frac{dT_a}{dt} = \alpha(T_o - T_a) - \gamma_a T_a + N_a, \quad \text{and} \qquad (1)$$

$$\frac{dT_o}{dt} = \beta(T_a - T_o) - \gamma_o T_o + N_o, \qquad (2)$$

where T_a is the near-surface atmospheric temperature, T_o is the SST, (α, β) are exchange coefficients normalized by the respective heat capacities of the atmosphere and ocean with $\beta \ll \alpha$, (γ_a, γ_o) are radiative damping coefficients, and (N_a, N_o) represent stochastic forcing arising from weather or turbulent eddies in the atmosphere and ocean, respectively.

Increasing ocean noise

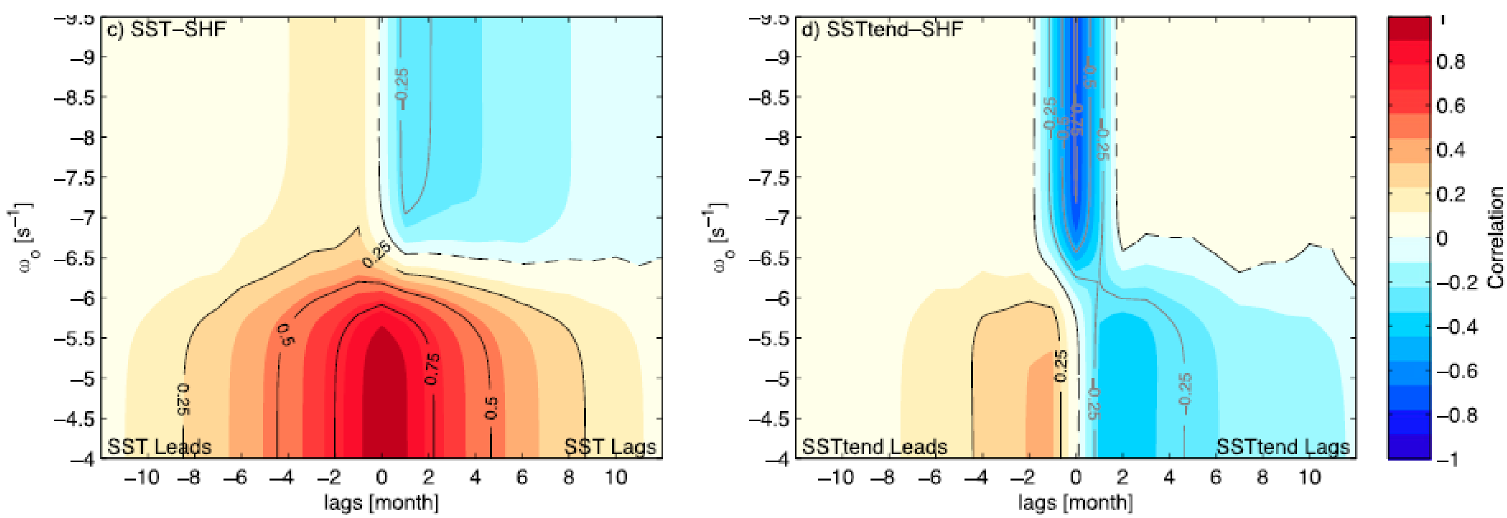

Increasing ocean noise

FIG. 1. Lagged correlations from solutions to the local energy balance model [Eqs. (1) and (2)]. (a) Lagged correlation between SST and SHF (blue) and between SST tendency and SHF (green) with variability driven by atmospheric noise. (b) As in (a), but with variability driven by oceanic noise. Lagged correlation between (c) SST and SHF and (d) SST tendency and SHF as a function of the forcing frequency ω_o of the stochastic ocean forcing N_o on a logarithmic scale. Black and gray contours are positive and negative correlations respectively [contour interval (ci) = 0.25] and the black dashed contour is the zero correlation contour. See appendix for details on the solutions to Eqs. (1) and (2).

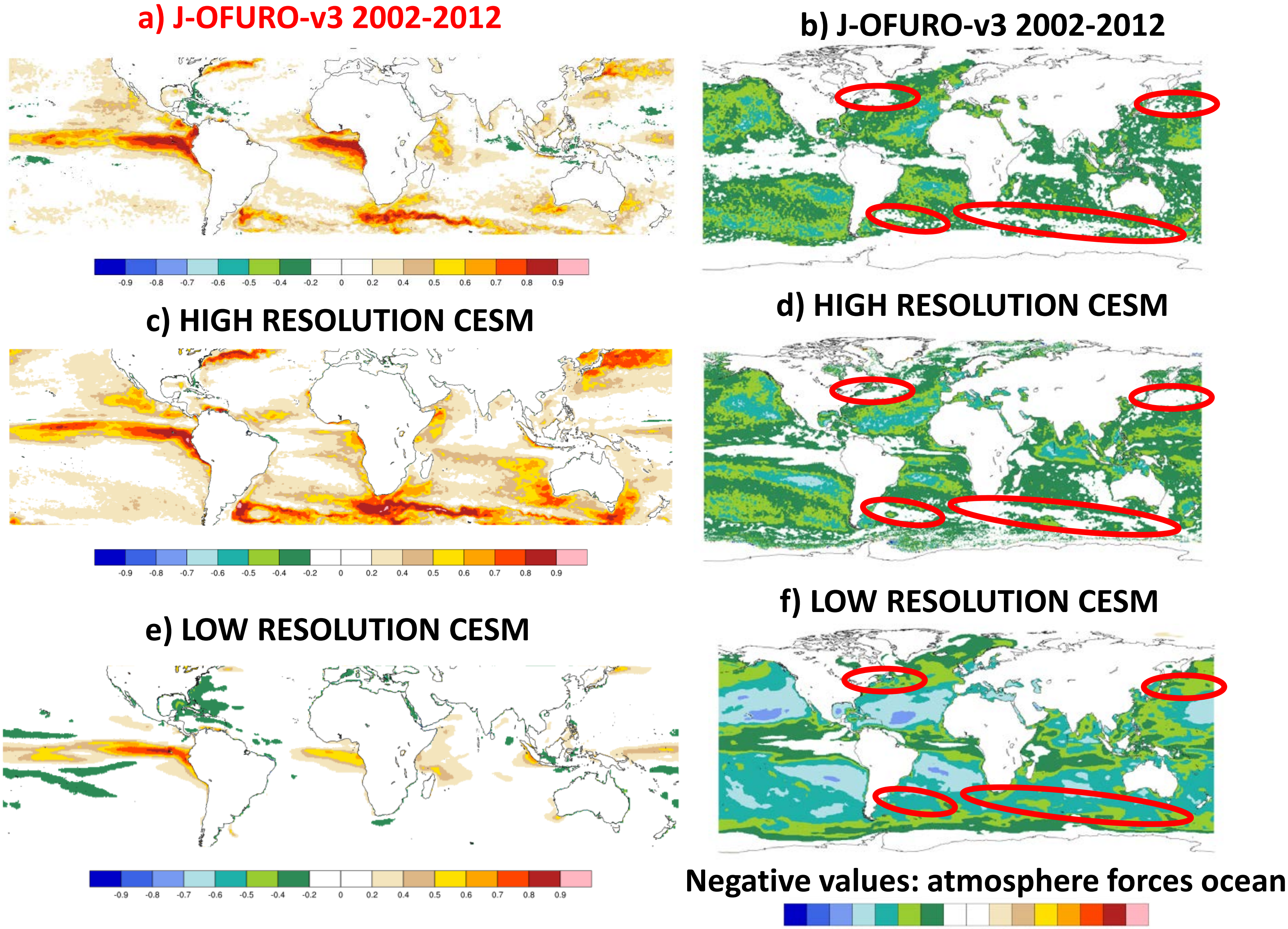

Left panels: correlation of SST and surface latent heat flux. Right panels: correlation of SST *tendency* and surface latent heat flux. Low resolution CESM much too atmosphere-driven.

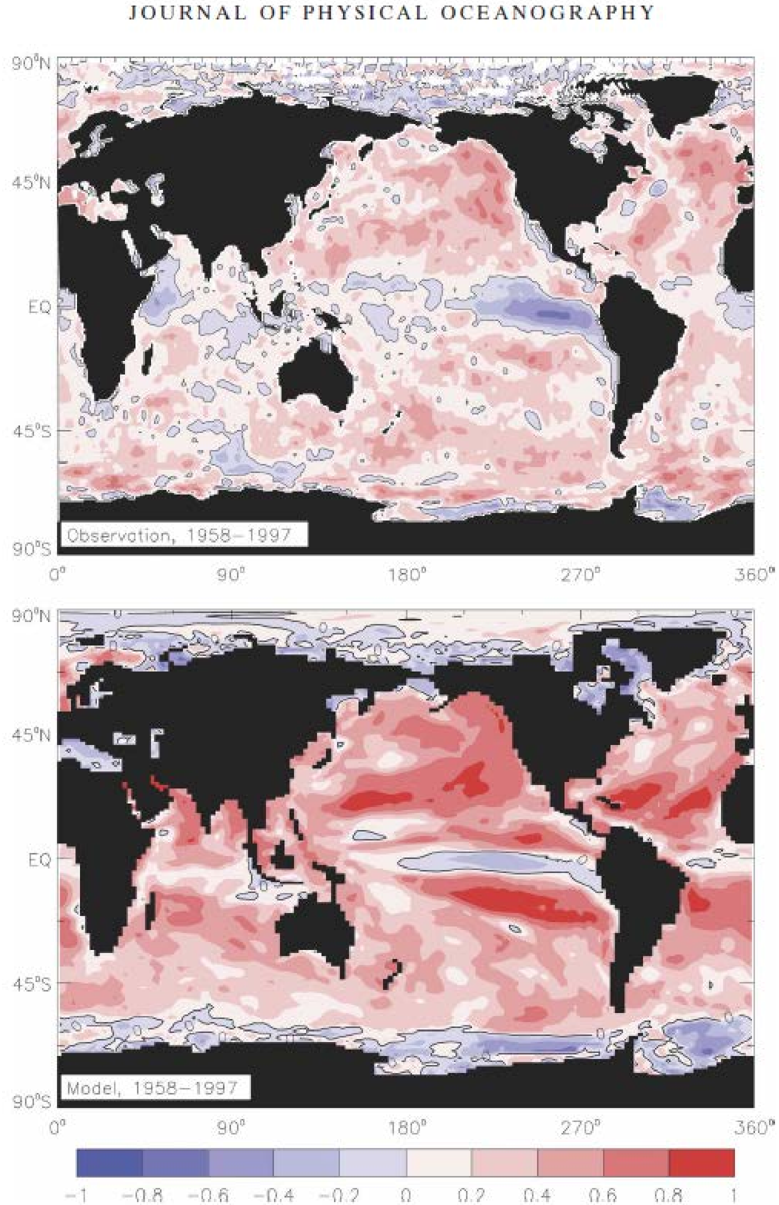

FIG. 4. Spatial distributions of the local correlation coefficient at each grid point between the annual average heat flux and change in SST over the corresponding year from the (top) observation record and the (bottom) model hindcast.

From Doney et al. 2007, analysis of hindcast simulations, **interannual variability**. Switched sign convention to right-hand-panels on previous slide.

Hindcast model is too much atmosphere-driven

Positive values: atmosphere forces ocean

Initial interpretation

- High-resolution model appears to be dominated by SST forcing of surface turbulent heat flux (THF)
  - Consistent with Barsugli&Battisti 98 model with incorporated strong ocean noise (Wu and Kirtman 2006, Bishop et al 2017)
- Low-resolution model appears to be dominated by a passive response of SST to THF
  - Consistent with B-B 98 model with strong atmosphere noise
- ***Is this the whole story? And what about deeper ocean heat content?***

Overview

- Approach
  - **Here we focus on short-term, monthly variability**
  - The monthly climatology and the linear trend is removed from the data, as are regressions on Nino3.4 SST.
  - **Will not consider low-frequency variability (e.g. Yeager et al. 2012, Clement et al. 2015, Zhang et al. 2017, Cane et al. 2017 etc.)**
  - Extratropics
  - Spatial maps of pointwise correlation or regression are shown
  - Two depth-averages chosen : to 50m, to 400m
  - The ocean temperature budget is analyzed
  - Results from a spatial smoother of budget terms shown
- Observations
  - **THF from OAFLUX (Yu and Weller 2007), J-OFUROv3 (Kubota et al 2001, Tomita et al. 2010), SEAFLUX (Curry et al 2001, C. A. Clayson)**
  - SSH from AVISO
  - SST from Reynolds et al. 2007
- Models
  - **CESM-HR. Coupled simulation with 0.1deg. ocean model.**
  - **CESM-LR. Coupled simulation with 1deg. ocean model.**
  - **Short (5-10 year) segments analyzed with full budget terms.**

Ocean heat budget to 50m

$$\rho c \int_{-D}^{0} \left(\frac{\partial T}{\partial t} + \underline{U} \cdot \nabla T - H_{diff} \right) dz = Q_s - Q_D$$

Tendency

3D resolved Advection or OHFC

Hor. Diffusion or GM advection

Net Surface heat flux

Vdiff

turbulent flux at depth D

- Following Doney et al. 2007, we regress the budget terms onto the total tendency
  - Values near +1 show a dominance of the term
  - Negative values counteract tendency
  - Positive values reinforce tendency

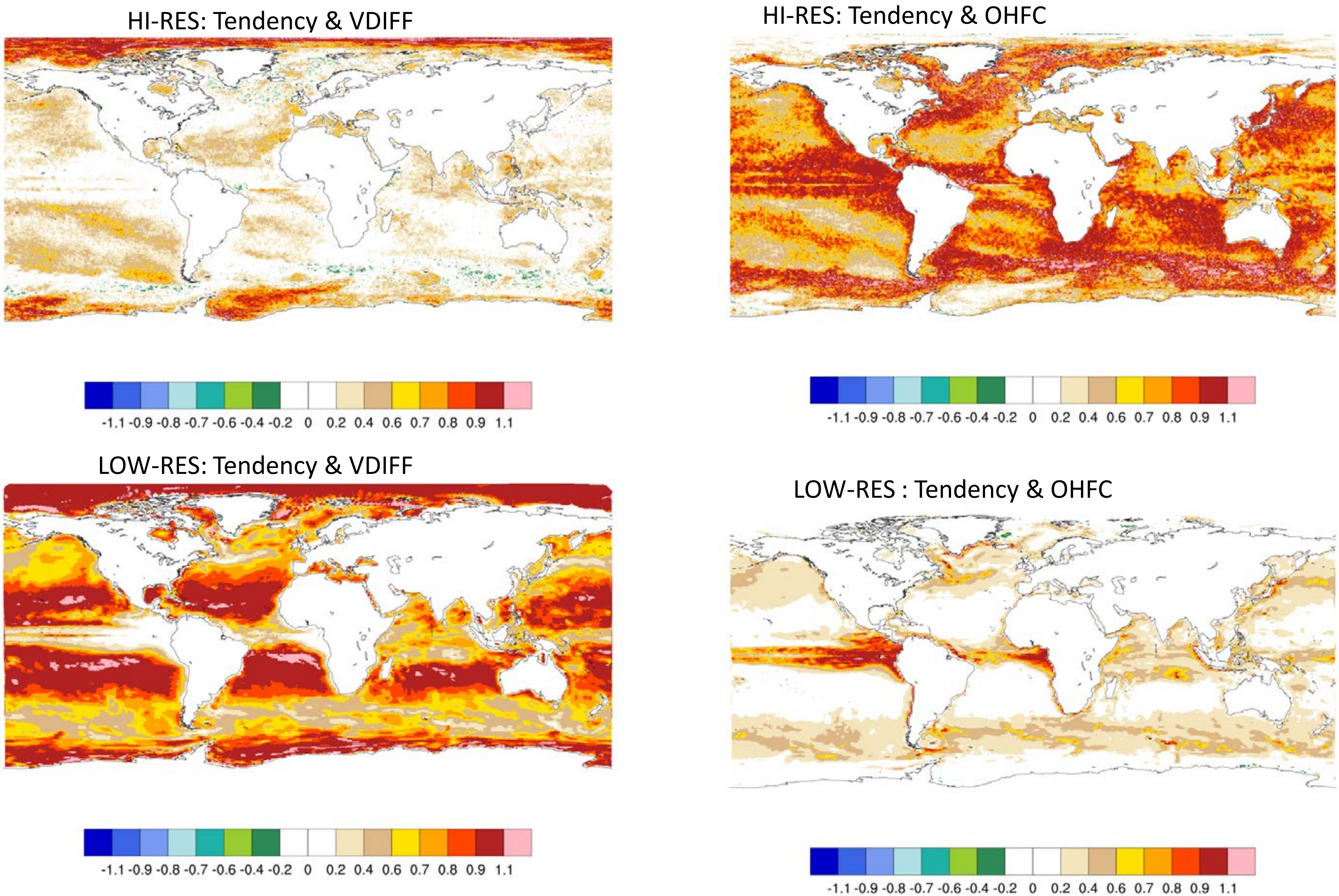

Fig. 14 Left panels: Regression of **vertical diffusion including surface heat flux** on heat content tendency and : to 50m. Right panels: Heat content tendency and **advection (or Ocean Heat Flux Convergence, OHFC)** : to 50m

LOW-RES : Correlation, Tendency & OHFC

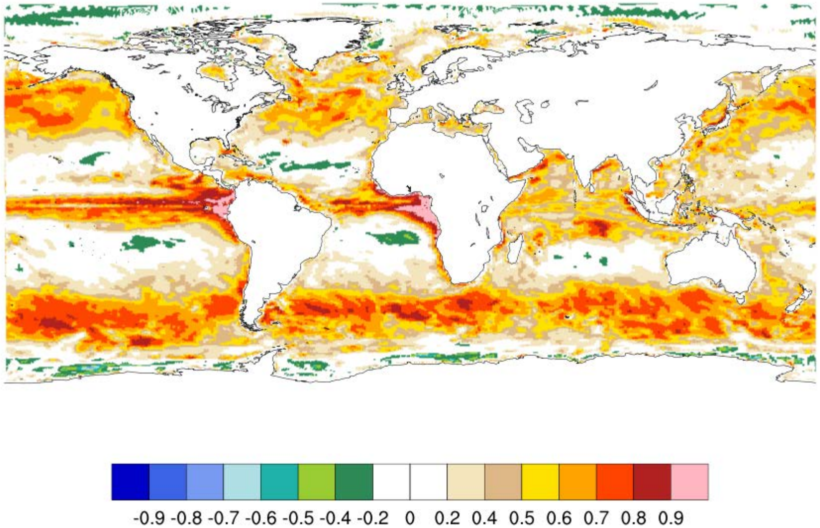

Correlation, temperature tendency to 50m and Ekman heat transport anomaly

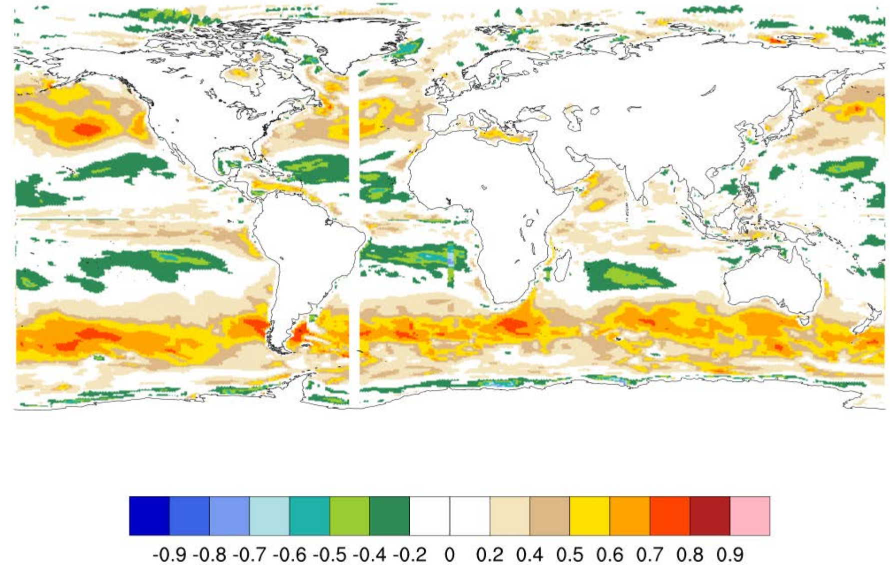

Correlation, full advection to 50m and Ekman heat transport anomaly

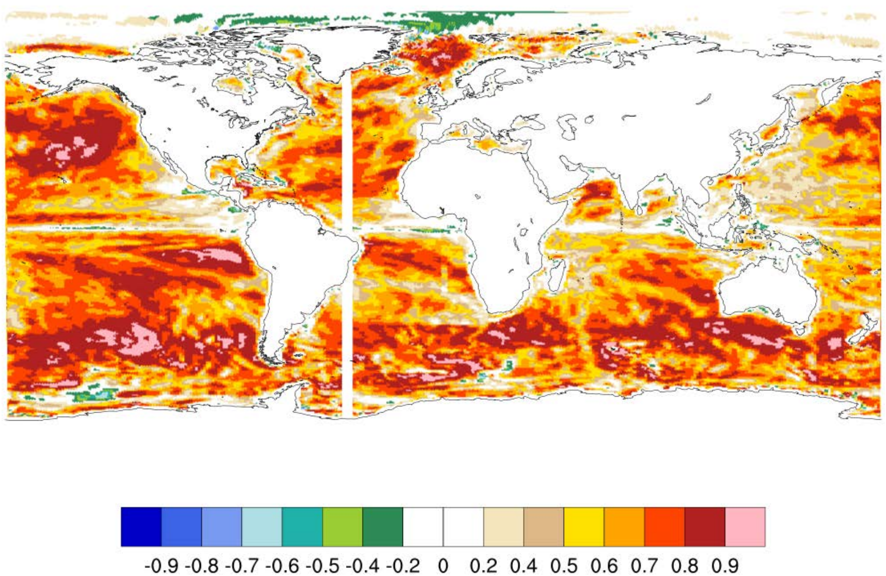

All results from low-resolution model

Ekman heat transport anomaly is written as

$$-\frac{\rho c_p}{\rho f}\left(\frac{\partial \overline{SST}}{\partial x}\tau_y{}' - \frac{\partial \overline{SST}}{\partial y}\tau_x{}'\right) - \frac{\rho c_p}{\rho f}\left(\frac{\partial SST'}{\partial x}\overline{\tau}_y - \frac{\partial SST'}{\partial y}\overline{\tau}_x\right)$$

Where overbars are climat. means, primes are deviation. I start from monthly data. The first set of brackets dominates. The whole expression is negated to be on RHS of temperature equation.

Figure 15. Role of Ekman advection

Ocean Heat budget to 400m

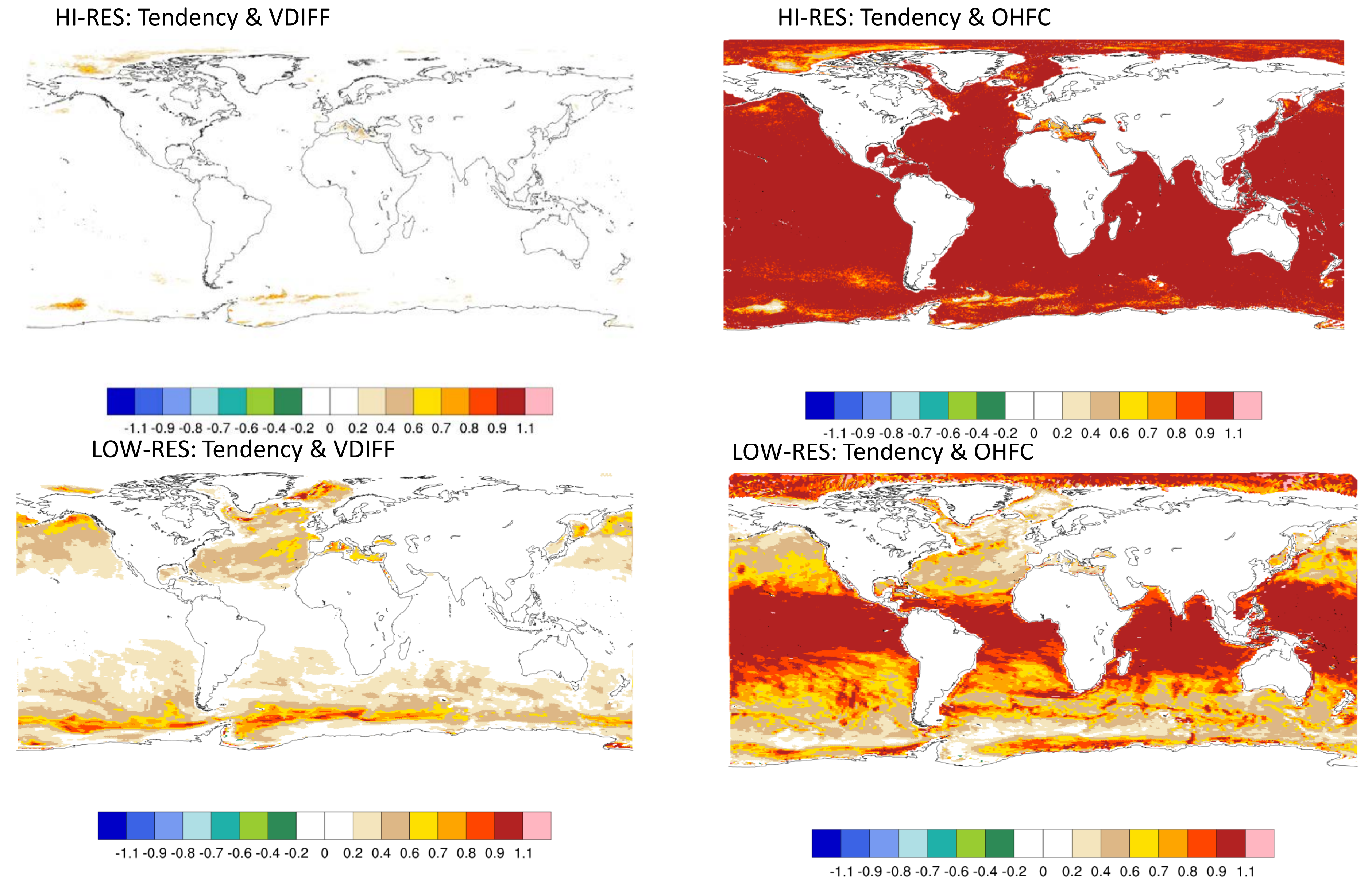

Fig. 16. As Fig. 14 but for a depth-integral to 426m.

Left panels: Regression of **vertical diffusion including surface heat flux** on heat content tendency . Right panels: Heat content tendency and **advection (or Ocean Heat Flux Convergence, OHFC)**

Scale-dependence

- The heat budget in the high-resolution model is clearly very different from that of the low-resolution model
  - Is one of the models wrong, are both wrong, or is it a question of spatial scale dependence?
- The heat budget terms from the high-resolution model are spatially smoothed with a box-car filter. Results are compared with low-resolution case.

Regression between heat content tendency and **vertical diffusion including surface heat flux**: to 50m.

Plots show HI-RES, LOW-RES, and HI-RES with various amounts of box-car smoothing. The full width of smoothing is labelled (1deg, 3deg etc).

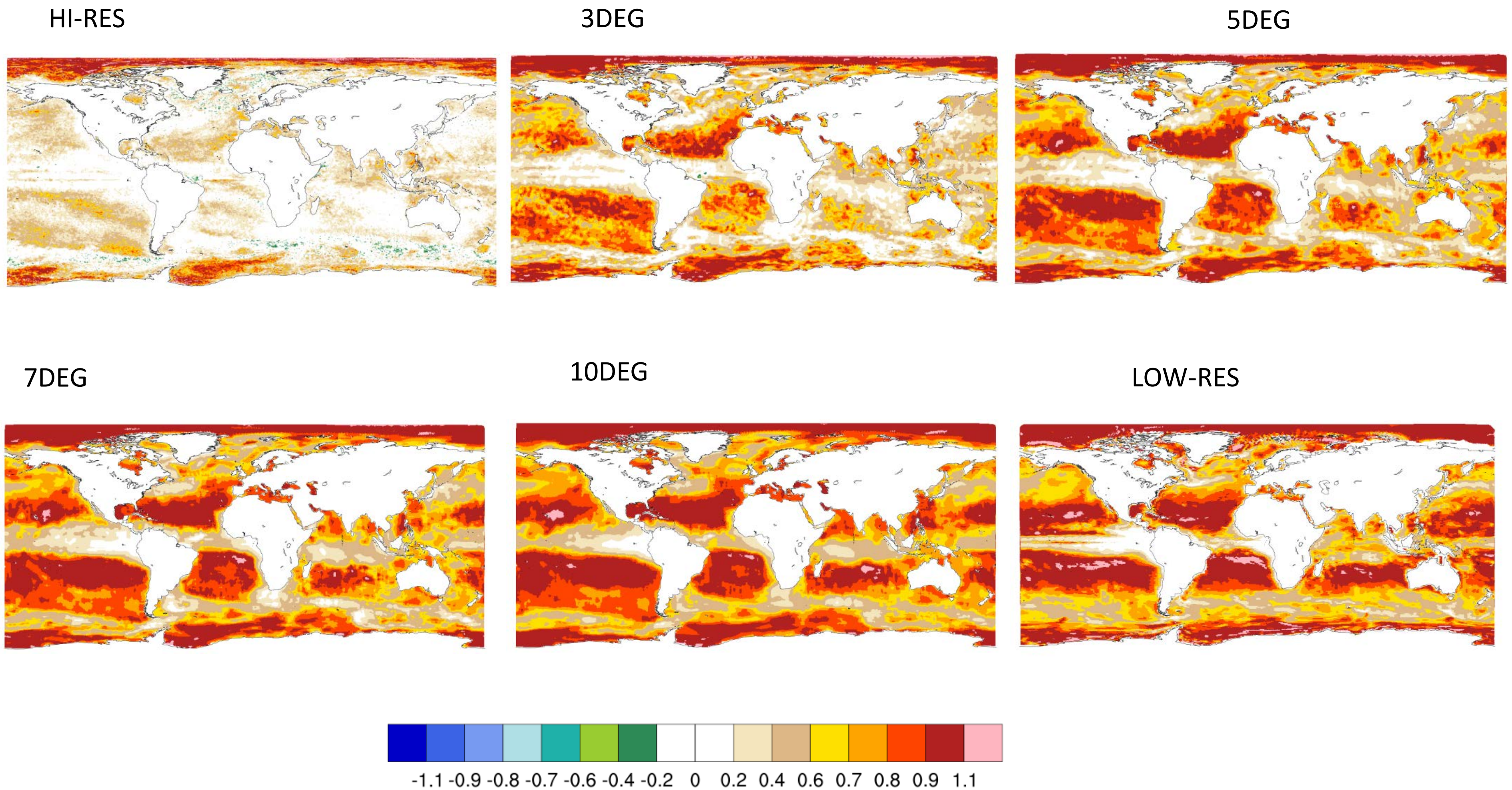

After about 7deg smoothing, high-res looks like low-res

Regression between heat content tendency and **advection**: to 50m.

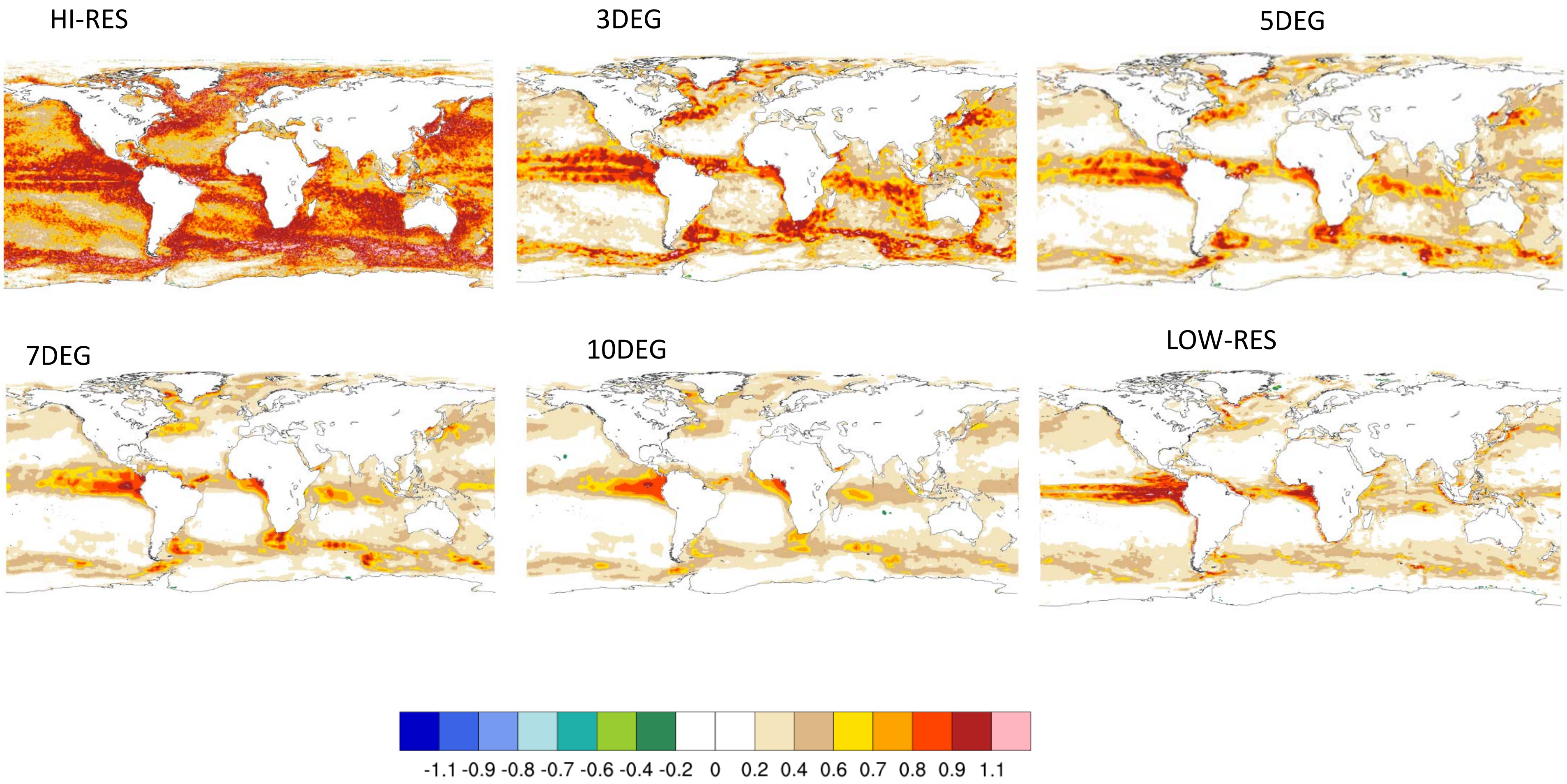

After about 7deg smoothing, high-res looks like low-res, and shows the structure of Ekman heat advection

Regression between heat content tendency and **vertical diffusion including surface heat flux**: to 400m.

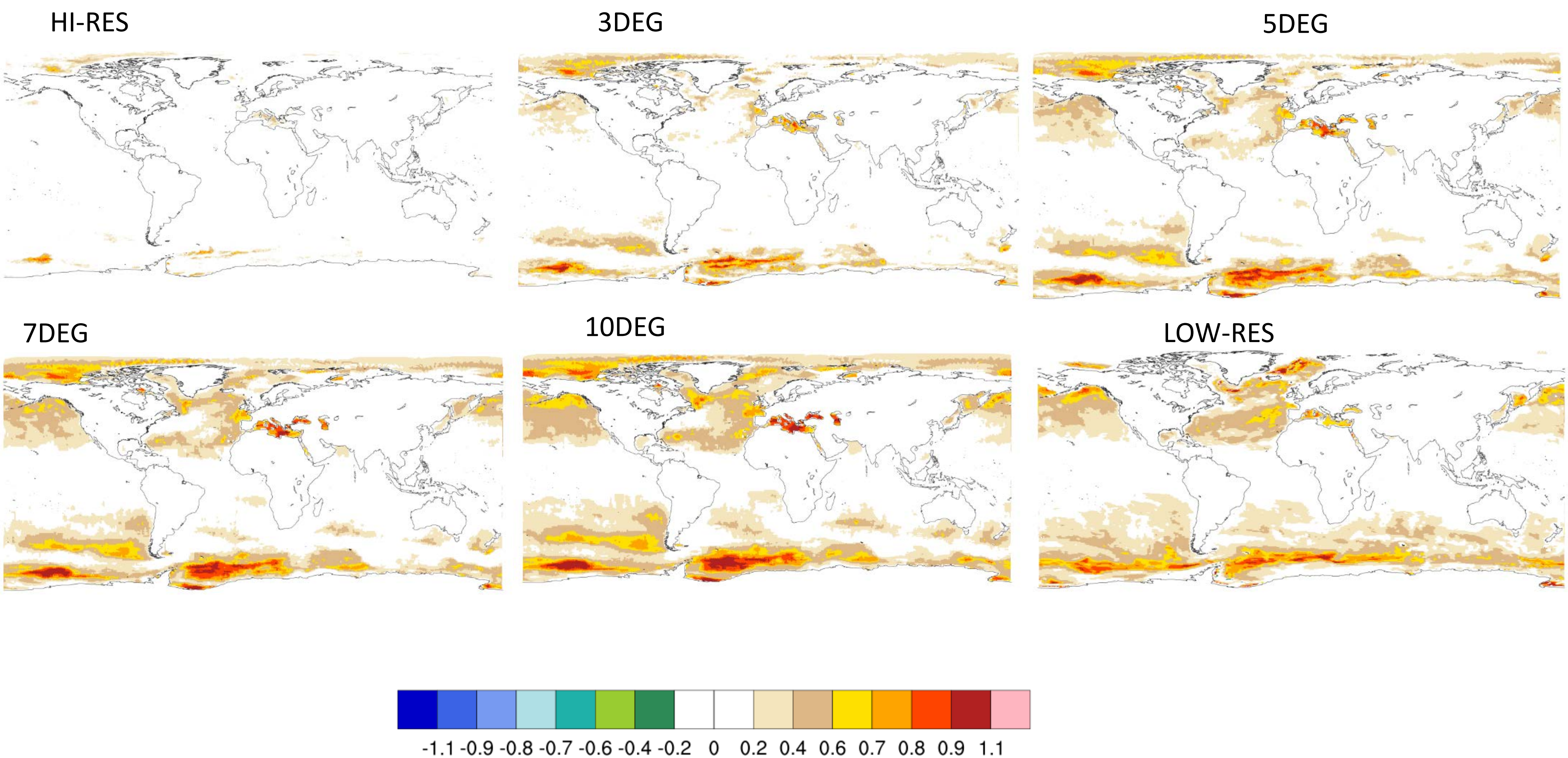

After about 10deg smoothing, high-res looks like low-res, except in frontal regions

Regression of Heat content tendency and **advection**: to 400m

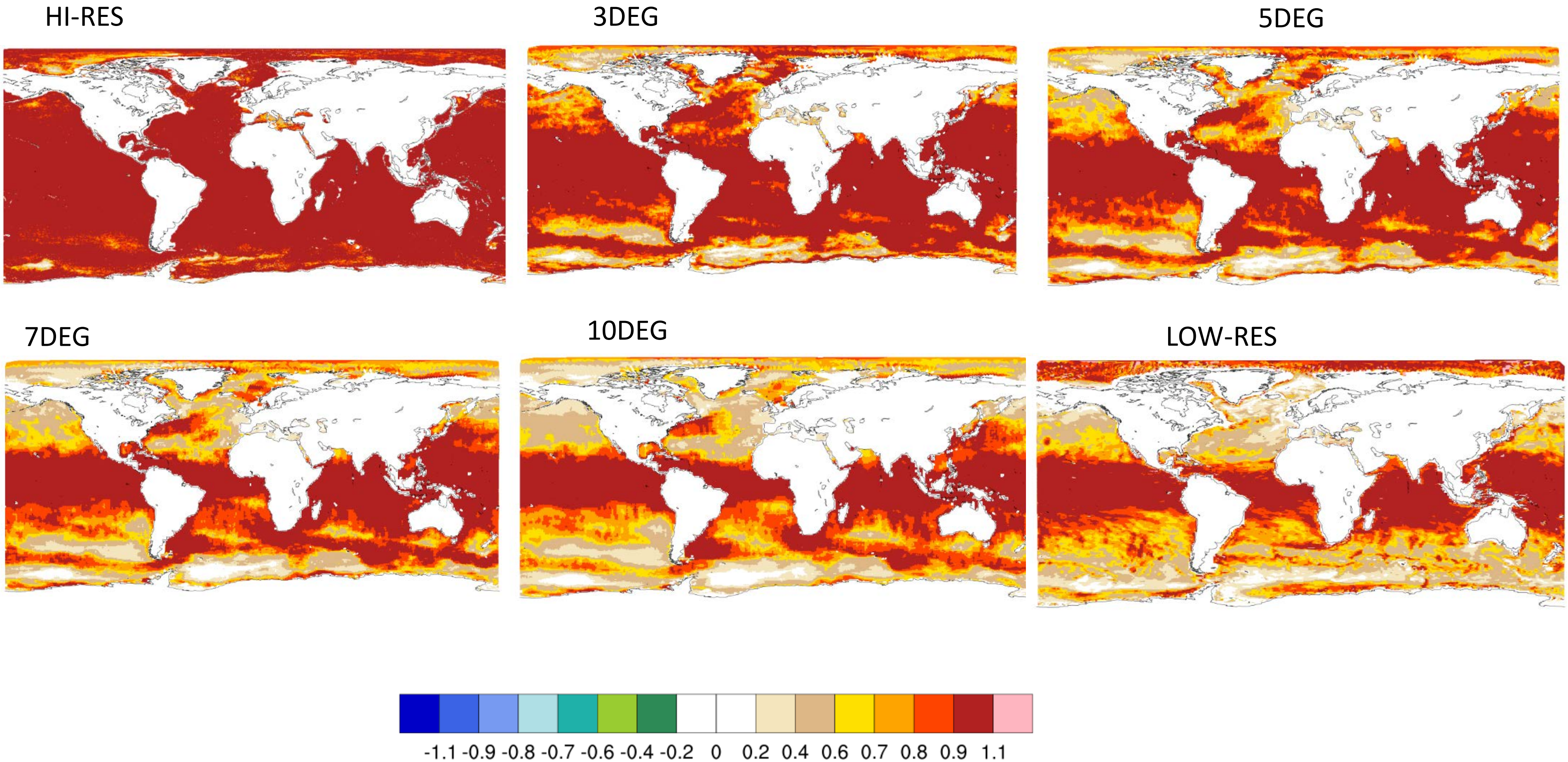

After about 10deg smoothing, high-res looks like low-res, except in frontal regions

Regression of Heat content tendency and vertical diffusion including **surface heat flux**: to **426m**

10DEG LOW-RES

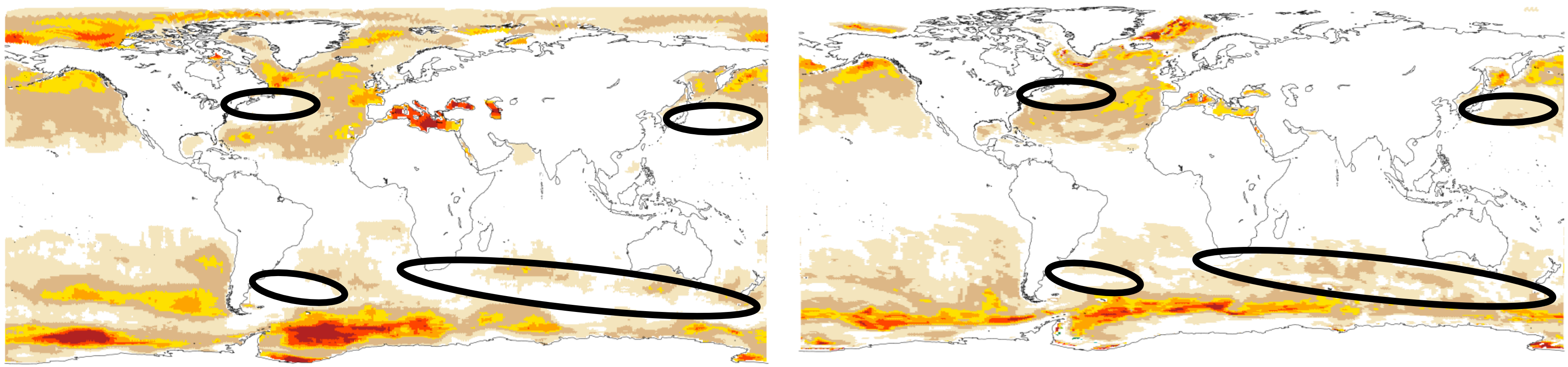

Regression of Heat content tendency and **advection**: to 426m

10DEG LOW-RES

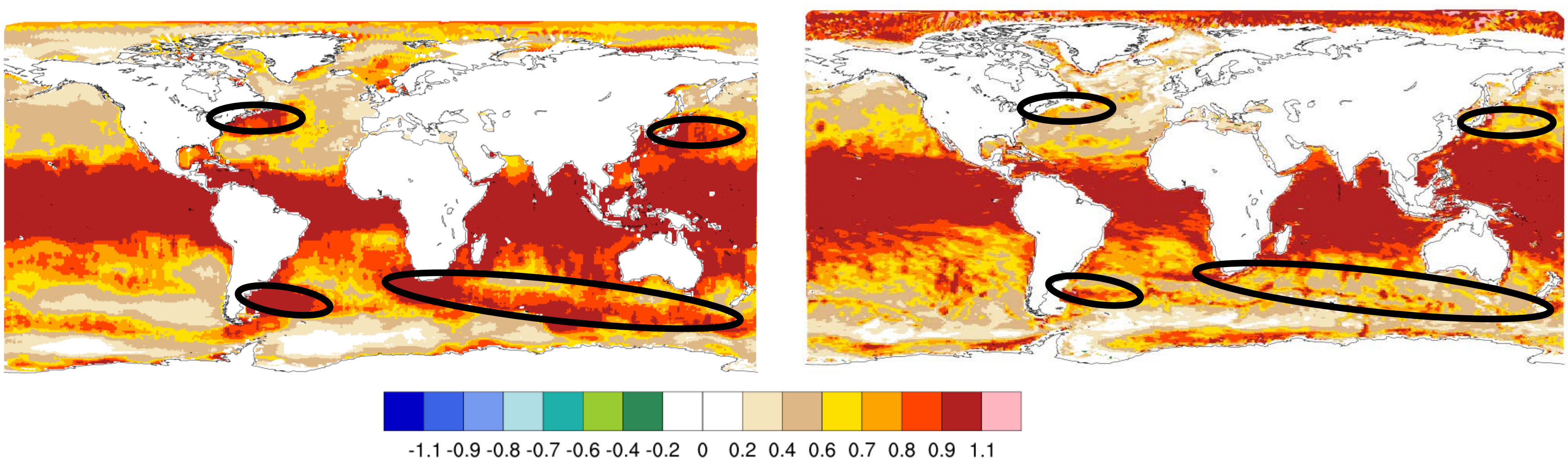

After about 10deg smoothing, high-res looks like low-res, except in frontal regions

Ocean intrinsic scales

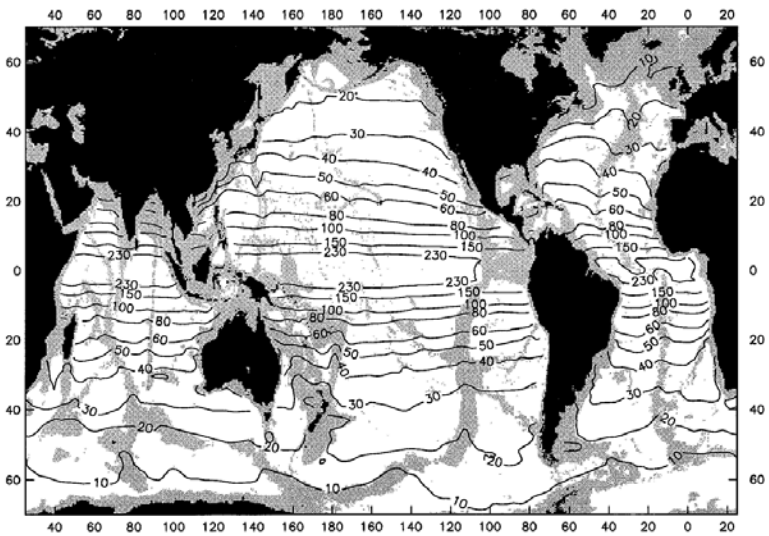

FIG. 6. Global contour map of the 1° × 1° first baroclinic Rossby radius of deformation λ_1 in kilometers computed by Eq. (2.3) from the first baroclinic gravity-wave phase speed shown in Fig. 2. Water depths shallower than 3500 m are shaded.

Chelton and deSzoeke et al 1998
First Linear baroclinic Rossby radius

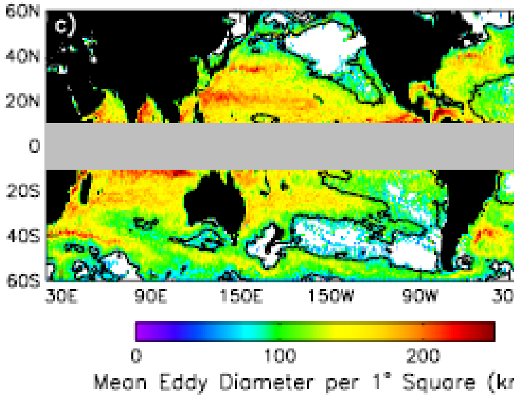

Chelton et al 2007

Eddy tracking method

Figure 3. The eddy characteristics in 1° squares for eddies with lifetimes ≥4 weeks: (a) The number of eddies of both polarities (white areas correspond to no observed eddies); (b) the mean amplitude; (c) the mean diameter; and (d) the percentage of SSH variance explained (white areas correspond to 0%). The contour in each panel is the 4 cm standard deviation of filtered SSH.

R. Hallberg / Ocean Modelling 72 (2013) 92–103 93

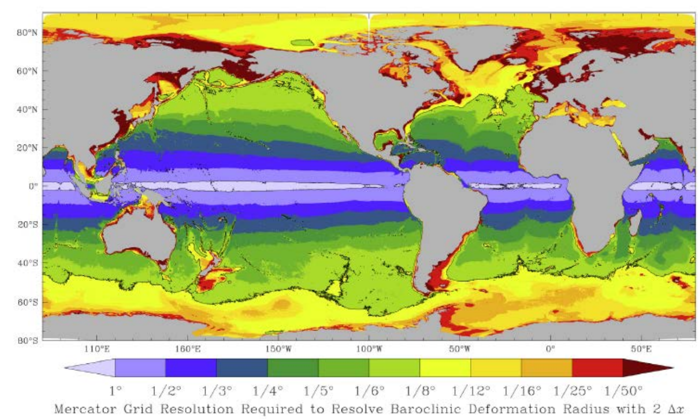

Fig. 1. The horizontal resolution needed to resolve the first baroclinic deformation radius with two grid points, based on a 1/8° model on a Mercator grid (Adcroft et al., 2010) on Jan. 1 after one year of spinup from climatology. (In the deep ocean the seasonal cycle of the deformation radius is weak, but it can be strong on continental shelves.) This model uses a bipolar Arctic cap north of 65°N. The solid line shows the contour where the deformation radius is resolved with two grid points at 1° and 1/8° resolutions.

Hallberg 2013. Model grid spacing required to “resolve” Rossby radius

10deg. Smoothing is not enough to reduce high-res model to atmosphere-driven in WBCs. But 10deg. Is much larger than typical eddy-scales – see plots on this page.

Conclusions ~~Initial interpretation~~

- High-resolution model **is** dominated by SST forcing of THF
  - **SST is driven by unforced advection variability on small scales of 5-10deg. or less**
  - **On larger scales it is similar to low-res, including the Ekman advection part**
  - excepting strong eddying regions in 400m depth-average
- Low-resolution model **is** a combination of a passive response of SST to THF and to Ekman (wind) variability
  - **THF forcing dominates in 50m average**
  - **advection (probably Ekman) dominates at 400m**
- Stochastic Barsugli-Battisti type model is limited as it does not include Ekman advection effect on ocean temperature

Background literature

- Stochastic models of air-sea interaction
  - Frankignoul, Hasselman 1977
  - Barsugli and Battisti 1998
  - Wu et al. 2006
  - Zhang et al 2017 – Bishop et al 2017
- Intrinsic ocean variability
  - (e.g. Serazin et al 2015, Nonaka et al 2016)
- Role of ocean heat transport convergence in observed ocean variability
  - (e.g.Doney et al 2007, Yeager et al 2012, Clement et al. 2015, Zhang et al. 2017, Roberts et al 2017)
- Role of local Ekman heat transport
  - (e.g.Doney et al 2007, Buckley et al. 2014, 2015, Larson et al., submitted)

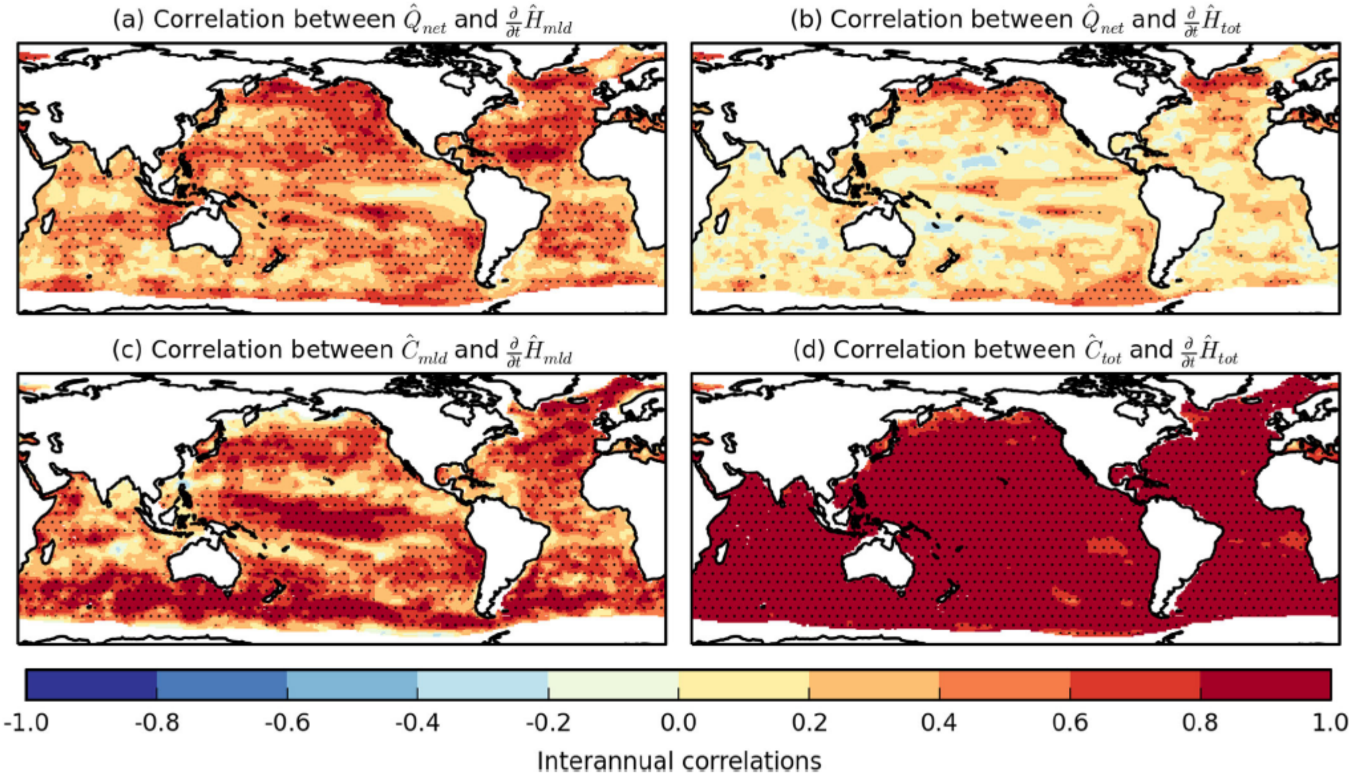

Figure 7. Correlations between different components of the interannual heat budget. Stippled areas indicate regions with $|r| \geq 0.374$, the critical value corresponding to $p = 0.05$ for a two-sided test assuming $N-2$ degrees of freedom, where $N = 28$.

Roberts et al 2017

$$\frac{\partial H}{\partial t} = C + Q_{net}$$

Heat content tendency = Heat transport convergence + Net surface heat flux

Observational study where C is computed as a residual.

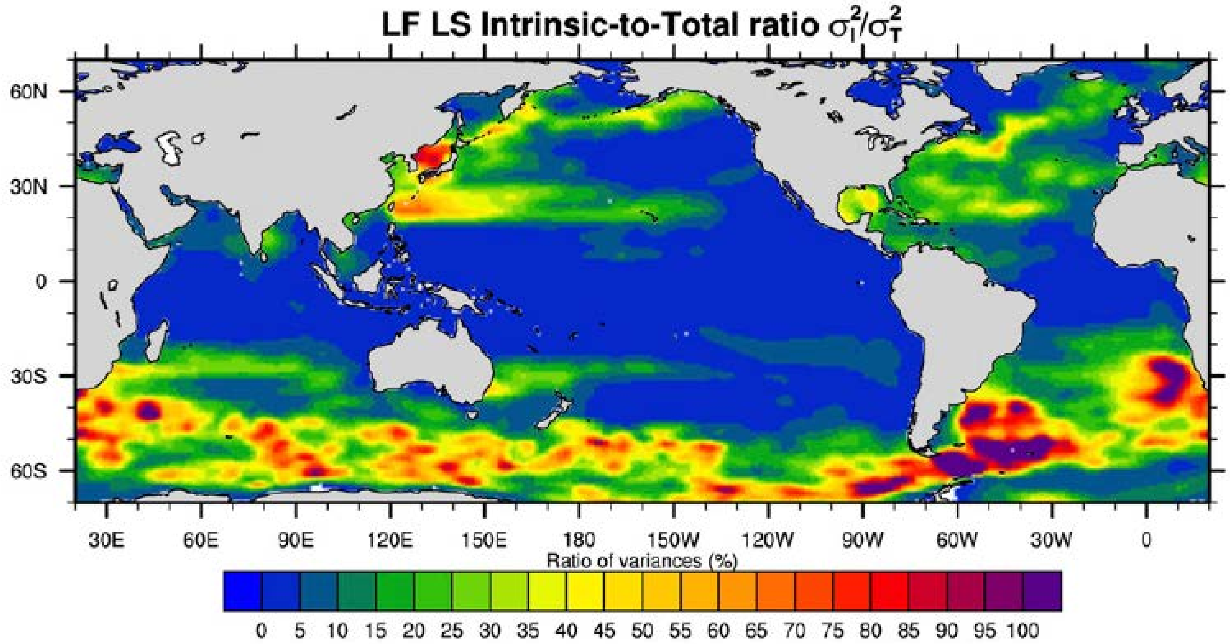

FIG. 8. As in Fig. 6, but at LFLS scales.

Intrinsic variability important to low frequency, large scale variability in S. Ocean and northern midlatitudes.

Sérazin et al, J. Clim 2015. Role of intrinsic ocean variability in sea level variability.

Obtained from forced ocean simulations, with either climatological forcing or time-varying forcing.

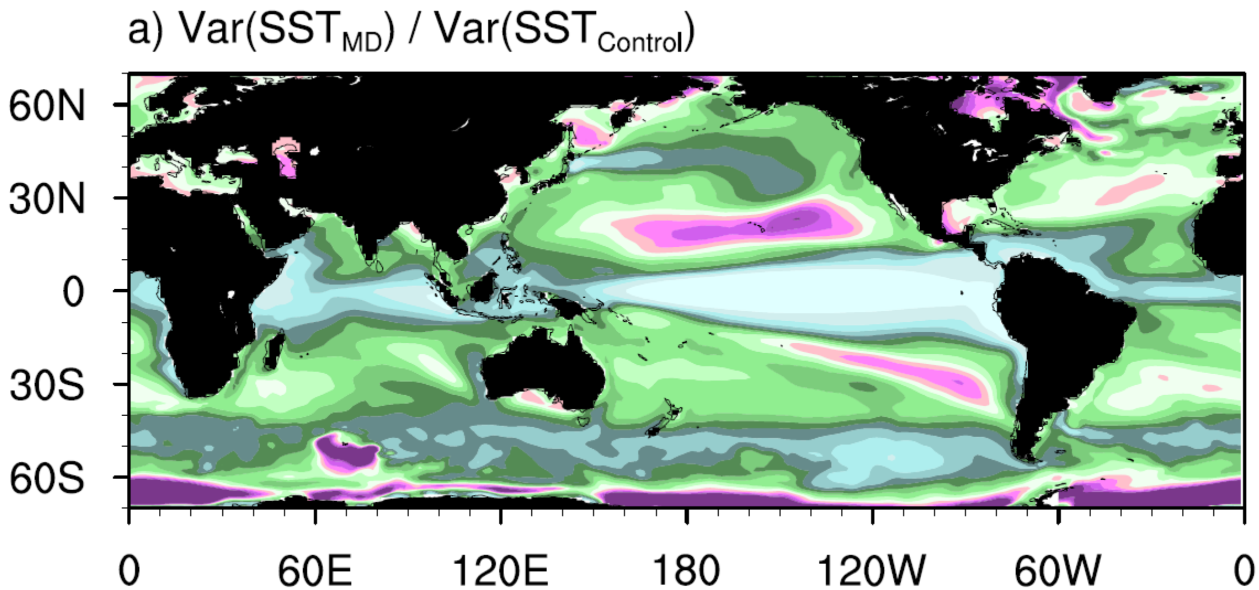

From Larson et. al. 2018, submitted

Figure 1. a) Unfiltered SSTA variance ratio VR_{SST} calculated as the variance of SSTA in the mechanically decoupled (MD) CESM divided by that of the CESM fully coupled control. Variance is computed over time at each grid point. Values > 1 (pinks) indicated increased variance in the MD.

Variance is significantly reduced when wind stress variability removed – Ekman advection removed – except in some subtropical regions

Mechanically decoupled CESM – ocean does not feel wind stress variability but does feel variability in air-sea buoyancy fluxes (Larson pers. comm. 2017)

Correlation, temperature tendency to 50m and Ekman heat transport anomaly

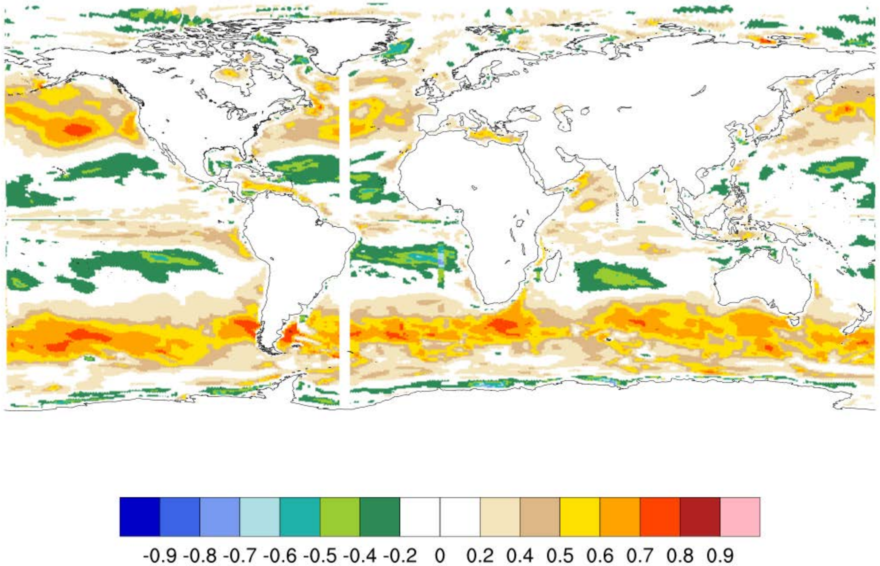

Correlation, temperature tendency to 426m and Ekman heat transport anomaly

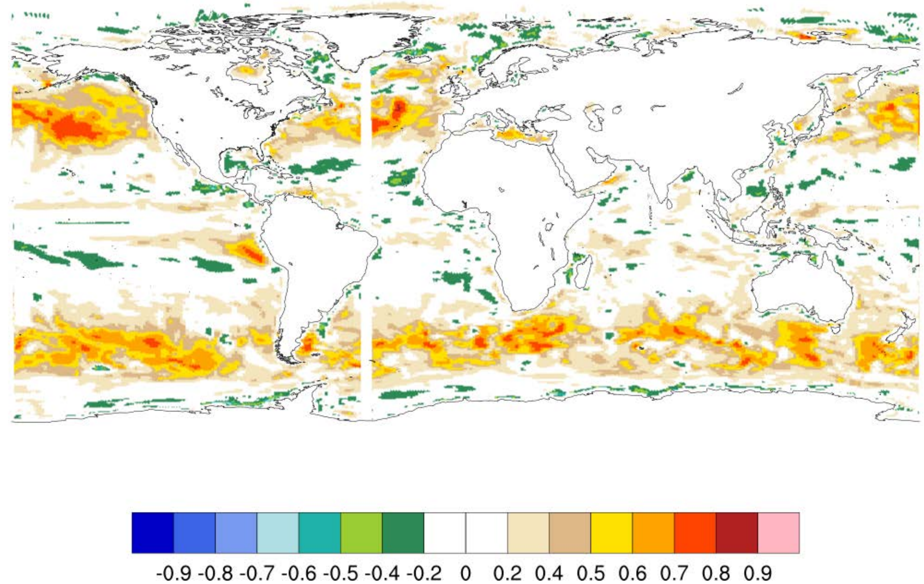

Correlation, full advection to 50m and Ekman heat transport anomaly

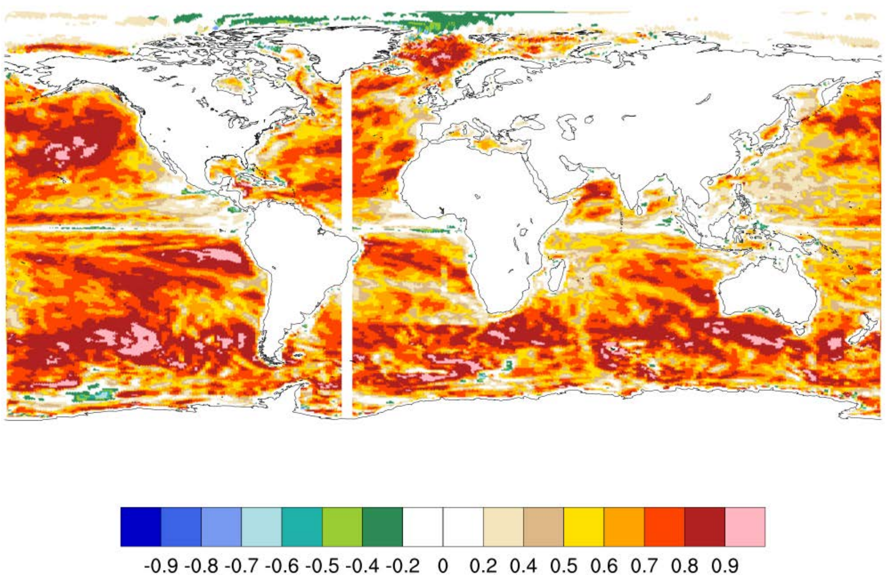

All results from low-resolution model

Ekman heat transport anomaly is written as

$$-\frac{\rho c_p}{\rho f}\left(\frac{\partial \overline{SST}}{\partial x}\tau_y' - \frac{\partial \overline{SST}}{\partial y}\tau_x'\right) - \frac{\rho c_p}{\rho f}\left(\frac{\partial SST'}{\partial x}\overline{\tau}_y - \frac{\partial SST'}{\partial y}\overline{\tau}_x\right)$$

Where overbars are climat. means, primes are deviation. I start from monthly data. The first set of brackets dominates. The whole expression is negated to be on RHS of temperature equation.

Figure 15. Role of Ekman advection

Low-res advection at 50m

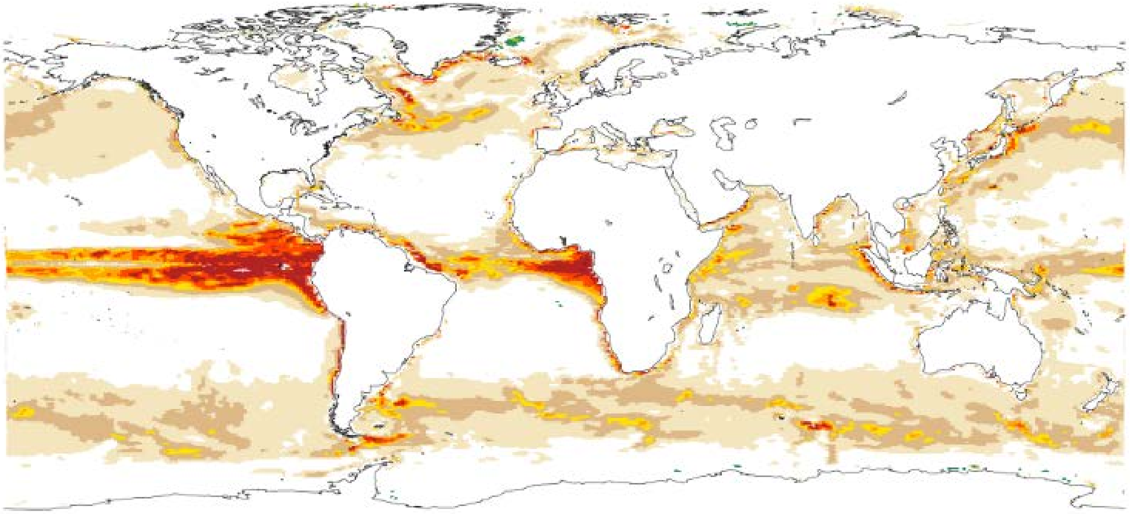

Low-res advection at 400m

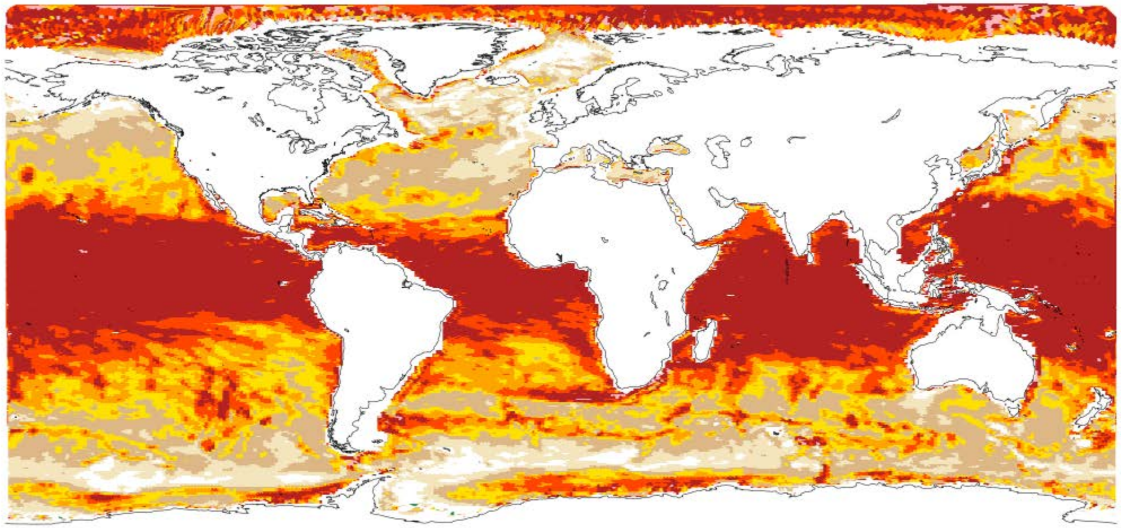

Recap: Correlation of SST and latent surface heat flux

a) OAFLUX 1993-2014

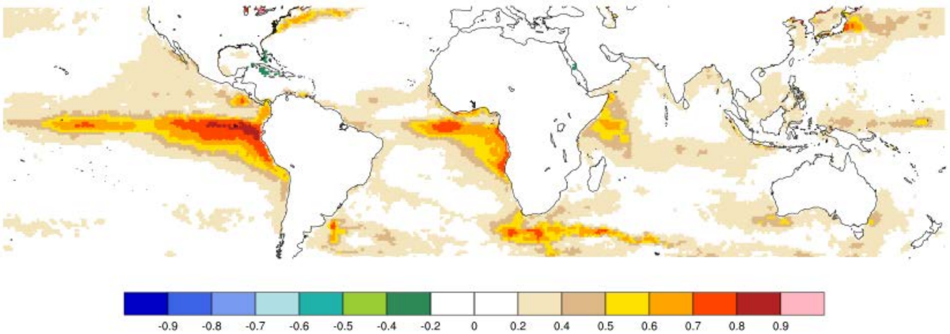

b) OAFLUX 2002-2012

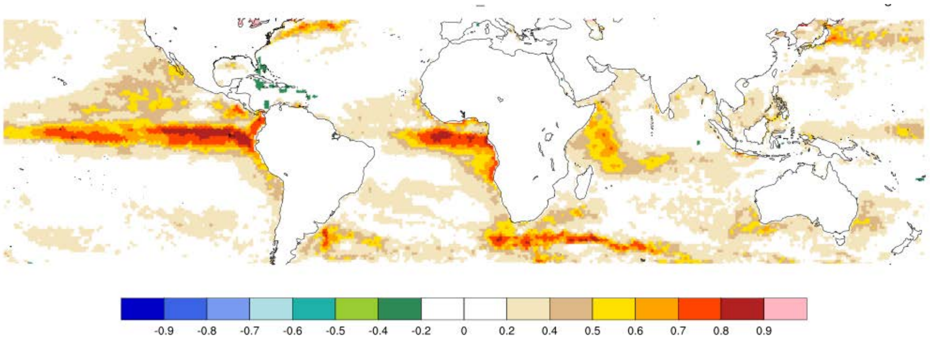

c) J-OFURO-v3 2002-2012

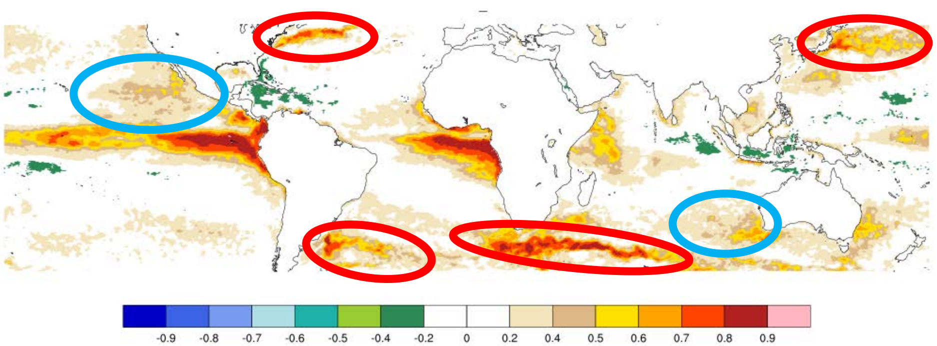

d) SEAFLUX 2002-2012

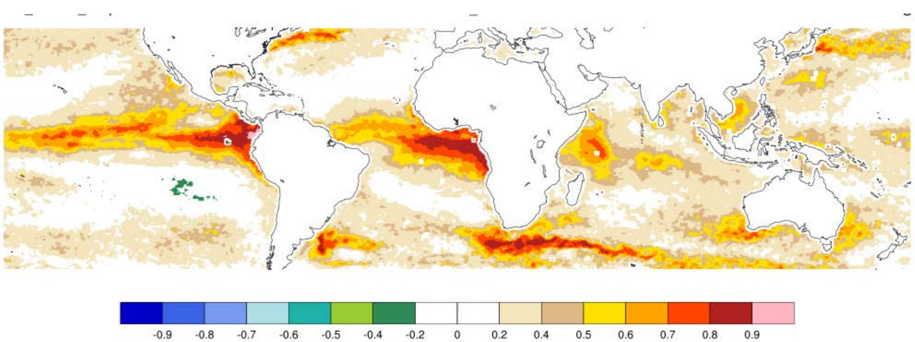

Positive values denote the ocean is not responding to surface heat fluxes: it is driving the surface heat fluxes

Strong positive correlations in ocean frontal/eddy regions (red circled) and also weaker ocean forcing in open ocean (e.g. blue circles) and Tropics

Correlation of SST and surface latent heat flux in **observational products**. Based on monthly data for period shown. Sign convention: positive surface heat flux is out of ocean.

SSH as a proxy for ocean heat content

Correlation SSH and THF

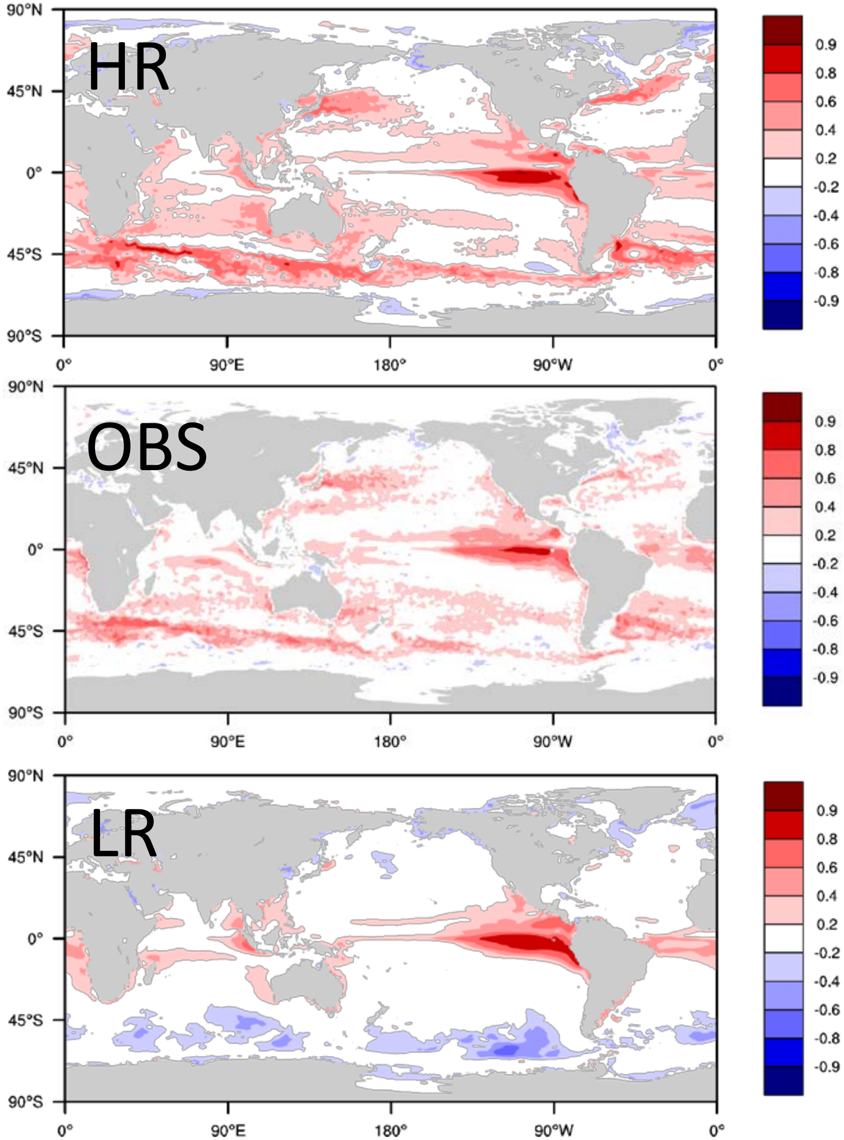

Correlation HC(400m) and THF

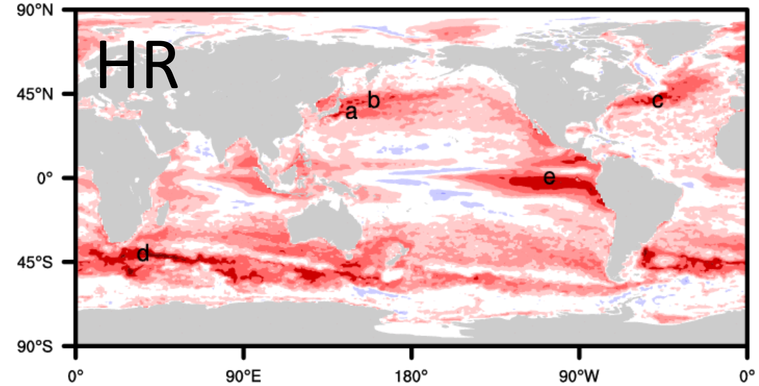

- Qualitative agreement in vicinity of WBC, ACC and other frontal regions